

Parent material influence on soil distribution and genesis in a Paleudult and Kandiuult complex, southeastern USA

J.N. Shaw^{a,*}, L.T. West^b, D.D. Bosch^c, C.C. Truman^c, D.S. Leigh^d

^a*Department of Agronomy and Soils, Auburn University, 202 Funchess Hall, Auburn, AL 36849, USA*

^b*Department of Crop and Soils, University of Georgia, 3111 Miller Plant Science Building, Athens, GA 30602, USA*

^c*USDA-SE Watershed Laboratory, P.O. Box 946, Tifton, GA 31794, USA*

^d*Department of Geography, University of Georgia, Athens, GA 30602, USA*

Received 12 March 2002; received in revised form 27 August 2003; accepted 16 October 2003

Abstract

Parent materials greatly influence soil development and the distribution of soils on the southeastern US Coastal Plain. We examined the physical, chemical, and mineralogical properties of 11 pedons in a 1-ha plot on the Upper Coastal Plain of Georgia, USA. Uniformity of parent materials was assessed by sand grain size characteristics. The soils have sandy epipedons of variable thickness and argillic horizons of variable texture. Six of the pedons also have kandic horizons. They are classified (US Soil Taxonomy) in Psammentic, Grossarenic, Arenic, and Typic subgroups of Paleudults and Kandiuults. Loamy pedons possess argillic horizons with two distinct increases in clay and greater differences between eluvial and illuvial horizons than sandy pedons. The upper boundary of the argillic horizon is approximately parallel to the present geomorphic surface, suggesting that it is associated with the contemporary surface. Discontinuities, identified by changes in sand grain size ratios and plots of the third (skewness) and fourth (kurtosis) moments of sand grain distribution, roughly correspond to the bottom of the solum. Our data suggest that there are both eolian and fluvial components in the solum, whereas subjacent horizons are completely derived from fluvial deposits. Sandier pedons have greater gibbsite/kaolinite ratios, possibly because greater permeability has enhanced leaching and Si loss. Our data suggest parent materials largely control soil distribution over this plot.

© 2003 Elsevier B.V. All rights reserved.

Keywords: Ultisols; Fluvial sediments; Eolian sediments; Argillic horizons

* Corresponding author. Fax: +1-334-844-3945.

E-mail address: jnshaw@acesag.auburn.edu (J.N. Shaw).

1. Introduction

Further understanding of soil-forming factors is necessary to develop models predicting soil distribution. Recently developed expert systems (e.g., [Zhu et al., 1997](#)) that integrate several data layers (e.g., geology maps) to map soil would be facilitated by improved understanding of the relationships between parent materials and soil patterns. However, the scale of observation and other factors often make these relationships difficult to evaluate.

Pedological investigations in the eastern and southeastern US Coastal Plain have evaluated parent material effects on soil genesis ([Gamble and Daniels, 1974](#)), the relationship between age of the geomorphic surface and soil morphology ([Daniels et al., 1970](#); [Markewich et al., 1986](#)), and the influence of eolian additions (loess) on soil type ([Rebertus, 1998](#)). Although fluvio-marine parent materials in the southeastern US greatly influence soil properties, few studies have evaluated the effects of short-range variation in these parent materials.

Portions of Georgia are ideal for investigating large-scale soil/parent material relationships because of the heterogeneity of parent materials. Pleistocene fluvial terraces are associated with present-day river valleys, and eolian processes have influenced the landscape. [Asmussen \(1971\)](#) suggested that these deposits were influenced by the pre-Quaternary drainage network and the direction of prevailing winds. Fluvial sediments tend to possess all grain sizes depending on source areas, energy, and gradients of flow; channel deposits are generally coarser than overbank sediments ([Davis, 1992](#)). In soils developed from fluvial parent materials, horizons rich in clay could be:

- 1) derived from overbank sediments (inherited from the parent material)
- 2) formed by mineral weathering and clay formation or translocation from overlying horizons, or
- 3) formed by some combination of both processes.

Eolian additions have also been recognized in some soils of the southeastern Coastal Plain. [Markewich and Markewich \(1994\)](#) reported Pleistocene dune sands on the leeward (east and northeast) side of major streams in the Coastal Plain of Georgia, and also recognized minor dunes along smaller streams. They also reported sands of mixed eolian and fluvial origin in soils farther leeward of the dunes. In contrast, [Leigh \(1998\)](#) suggested that surficial sands previously suspected as eolian at five sites in the Upper Coastal Plain of South Carolina were predominantly fluvial. In areas without distinctive dune morphology, the distinction between eolian and fluvial sands in epipedons has been based on their size, shape, and sorting characteristics ([Friedman, 1961, 1979](#); [Green, 1974](#); [Mazzulo and Ehrlich, 1983](#); [Bui et al., 1989](#); [Leigh, 1998](#)). However, eolian and fluvial sands often have overlapping grain size distributions ([Friedman, 1979](#); [Mazzulo and Ehrlich, 1983](#); [Bui et al., 1989](#)), and particle shape can be modified by weathering ([Green, 1974](#)).

One technique for differentiating eolian from fluvial deposits in near-surface sandy horizons has been to express the sand grain size distributions on a ϕ scale ($\phi = -\log_2 D$; D = grain diameter, in millimeters) and to evaluate the arithmetic moments of the size distribution, including the mean, standard deviation (S.D.; sorting), skewness, and kurtosis ([Friedman, 1961](#); [Leigh, 1998](#)). Both fluvial and eolian sands tend to be positively skewed,

which complicates their separation, but separates them from beach sands. However, because of differences in transportation mechanisms, fluvial sands tend to be coarser and less well sorted than eolian sands (Friedman, 1979; Bui et al., 1989).

In this paper, we attempt to assess parent material origins and their influence on soil properties in profiles affected by both fluvial and eolian processes in the Upper Coastal Plain of Georgia. We chose a site with a relatively high degree of short-range soil variability. The specific objective was to evaluate pedogenic and lithogenic influences on the Paleudults and Kandiodults occurring on the site.

2. Materials and methods

The study site is in the southern portion of the Fall Line Hills region near Plains, GA ($31^{\circ}59'0''\text{N}$; $84^{\circ}24'0''\text{W}$). The surface sediments are believed to be mostly Pleistocene fluvial deposits on a narrow terrace bounded on the west by the third order Ty Ty Creek, and on the east by a first-order tributary (Fig. 1). The terrace narrows from

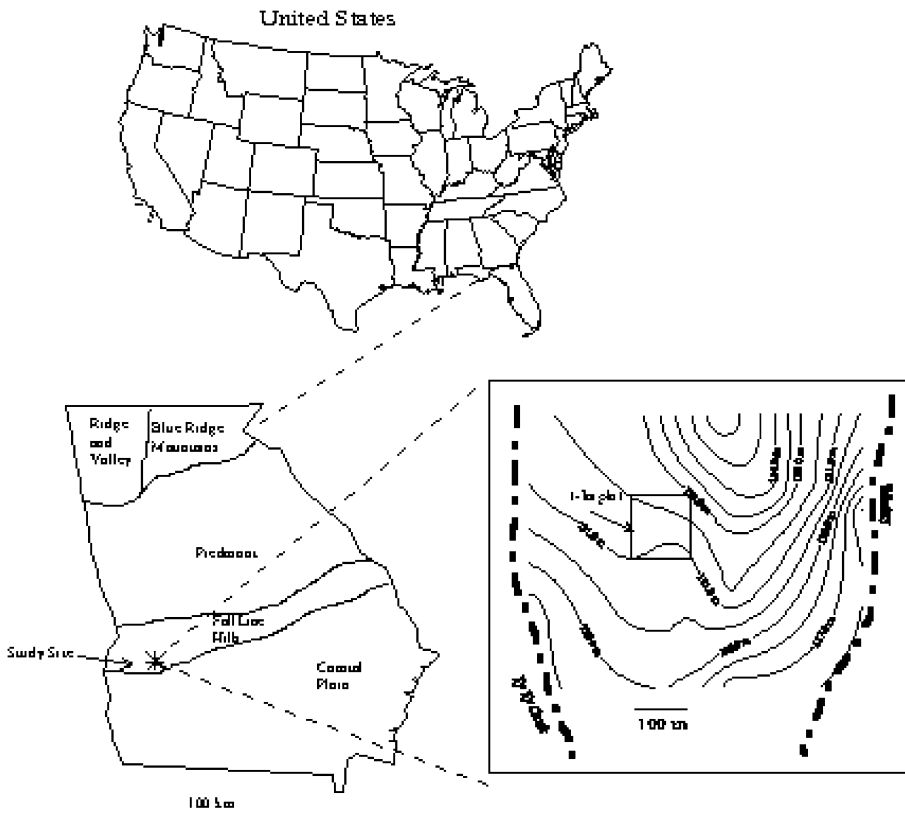


Fig. 1. Location of study site in Georgia, USA. Inset shows plot location.

north to south (where Ty Ty Creek and the tributary join), with an interstream width of approximately 1 km near the study zone. The surface slopes to the south at approximately 3 m km^{-1} on the summit.

A 1-ha plot was established containing soils exhibiting the full range of characteristics for this landscape (Bosch and West, 1998). In the plot, sediments were sampled from eight borings to a depth of 10 m (A–H), and from three pits (NW, SE, and NE) at the corners of the plot (Fig. 2). Elevations were measured at the borings and several locations around the plot. Pedons NW and SE were analyzed most intensively as they exhibited large differences in soil properties. Pedons were described, sampled by horizon, and classified according to standard techniques (Schoeneberger et al., 1998). A transect was established inside the plot from the NW to the SE corner (Fig. 2), and at 5-m intervals, the soils were sampled at depths of 0.25, 0.50, 1.4, and 2 m (Bosch and West, 1998).

Bulk samples were air-dried and weighed, and coarse fragments were removed by crushing the samples and dry sieving through a 2-mm sieve. Particle size distribution (PSD) was determined on all plot and transect samples by the pipette method after removal of organic matter with H_2O_2 (surface horizons) and dispersion with sodium hexameta-phosphate (Kilmer and Alexander, 1949). Sand grains were separated into standard size fractions (1–2, 0.5–1, 0.25–0.5, 0.1–0.25, and 0.05–0.1 mm) by sieving. Fine clay ($<0.2 \mu\text{m}$) was measured for selected pedons (SE, NW, A, and H) by centrifugation and pipetting (Jackson, 1975). Basic cations were extracted with 1 M NH_4OAC (pH 7) using an autoextractor (Soil Survey Investigations Staff, 1996, p. 203–206), and measured by atomic absorption spectroscopy (AAS). Cation exchange capacity (CEC) of selected

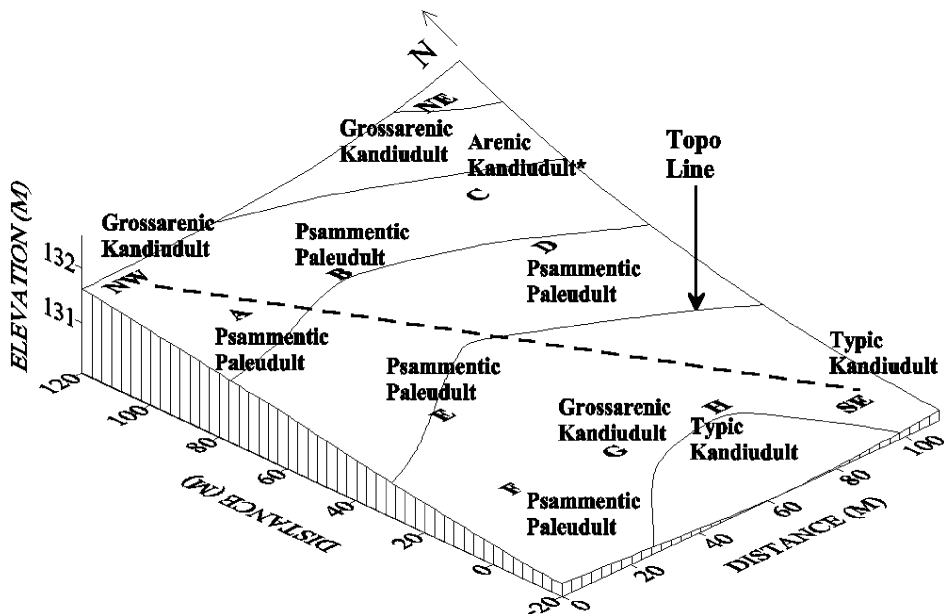


Fig. 2. Plot topography, location of sampling sites, soil classification, and the location of the transect inside the plot. Contour lines are at 0.5-m intervals. *Denotes cation exchange capacity not measured.

pedons was measured by the 1 M NH_4OAC (pH 7) method, and NH_4 was measured colorimetrically (Soil Survey Investigations Staff, 1996, p. 203–206). Aluminum was extracted with 1 M KCl using an autoextractor, and was measured by AAS (Soil Survey Investigations Staff, 1996, p. 259–263). Fe was extracted with acid ammonium oxalate (Fe_o) to measure poorly crystalline forms of free Fe, and with dithionite–citrate–bicarbonate (Fe_d) for crystalline Fe oxides (Jackson et al., 1986). The extracted Fe was quantified by AAS.

Sand grain size (0.05–2 mm) was measured on horizons from the NW and SE pedons using image analysis techniques. A video camera was mounted on a petrographic microscope, and grains were placed on a photographic gray card to optimize contrast. Sand grains were separated on the gray card to ensure that no particles were touching. Video images were captured and digitized to determine area, and equivalent grain diameters were calculated from the measured areas. Grain diameters were expressed on a Φ scale, and the size distribution moments (mean, standard deviation, skewness, and kurtosis) were calculated as follows:

$$\text{mean} = \frac{1}{n} \sum x_j \quad (1)$$

$$\text{S.D.} = \sqrt{\frac{n \sum x^2 - (\sum x)^2}{n(n-1)}} \quad (2)$$

$$\text{skewness} = \frac{n}{(n-1)(n-2)} \sum \left(\frac{x_j - x_{\text{avg}}}{s} \right)^3 \quad (3)$$

$$\text{kurtosis} = \left\{ \frac{n(n+1)}{(n-1)(n-2)(n-3)} \sum \left(\frac{x_j - x_{\text{avg}}}{s} \right)^4 \right\} - \frac{3(n-1)^2}{(n-2)(n-3)} \quad (4)$$

where n = number of observations, x_j = observation, x_{avg} = mean for all observations, and s = standard deviation. The coefficient of variation (CV) was calculated as s/x_{avg} .

Soil samples were fractionated by size following organic matter and Fe removal using standard techniques (Jackson, 1975). Gibbsite and kaolinite were determined in Mg-saturated clay fractions by differential scanning calorimetry (DSC). The temperature was increased from 100 to 600 °C at a constant rate of 10 °C min^{-1} , with an empty Al pan as a reference. These analyses were conducted in an N atmosphere to minimize oxidation. Kaolinite and gibbsite quantities were determined by integrating endotherms and comparison with endotherms for samples of known composition (Tan et al., 1986). Clay samples were oriented on glass slides using the method of Drever (1973) and examined by X-ray diffraction (XRD) after the following treatments: Mg saturation, glycerol solvation, and 25 °C; K saturation and 25, 300, and 550 °C (Whittig and Allardice, 1986). Sand fractions were pulverized in a ball mill grinder, and randomly oriented powders were examined by XRD. All XRD analyses utilized $\text{Cu-K}\alpha$ radiation and a graphite monochromator with a θ compensating slit; scan speeds were 2° 2θ min^{-1} . Hydroxy-interlayered vermiculite (HIV) quantities were estimated by the techniques of Karathanasis and

Table 1
Selected soil properties for six representative pedons on the site^a

Horizon	Depth (cm)	Color	Sand (%)	Silt (%)	Clay (%)	Fe _o /Fe _d ratio per 100 g of clay	CEC (cmol _c kg ⁻¹)	ECEC clay (cmol _c kg ⁻¹)	VC sand (%)
<i>NW: loamy, kaolinitic, thermic Grossarenic Kandiuult</i>									
Ap	0–12	7.5YR 4/4	90.6	6.0	3.4	5.02	54.6	31.8	3.6
A/E	12–26	7.5YR 4/4	90.8	6.7	2.5	5.21	57.5	16.4	4.7
E1	26–75	2.5YR 4/8	89.7	6.3	4.1	2.22	21.7	6.4	4.7
E2	75–109	2.5YR 4/8	89.3	6.4	4.4	–	19.2	–	5.1
E3	109–138	2.5YR 4/8	88.3	5.9	5.8	1.46	15.4	11.7	3.7
Bt1	138–191	2.5YR 4/8	81.0	3.8	15.2	0.44	14.1	7.4	5.3
Bt2	191–246	2.5YR 4/8	82.8	3.1	14.1	0.62	7.9	6.7	5.4
BC	246–300	2.5YR 4/8	87.9	2.4	9.7	0.72	8.3	3.9	7.1
CB	300–366	2.5YR 3/6	89.2	3.0	7.8	0.72	9.1	6.6	3.8
C1	366–434	10R 4/8	92.4	1.2	6.4	1.27	9.2	6.3	2.6
C2	434–466	10R 4/8	89.3	5.1	5.6	1.49	9.8	11.6	6.3
<i>SE: coarse-loamy, kaolinitic, thermic Typic Kandiuult</i>									
Ap	0–21	7.5YR 4/6	84.9	12.4	2.7	2.90	83.9	29.3	2.0
Bt1	21–52	2.5YR 4/6	77.1	11.3	11.6	0.22	17.3	7.0	1.0
Bt2	52–92	2.5YR 4/6	75.9	10.9	13.2	0.17	16.3	6.7	2.0
Bt3	92–126	10R 4/6	75.3	8.4	16.3	0.16	15.4	8.2	2.6
Bt4	126–164	10R 4/6	66.1	5.8	28.1	0.24	11.1	6.7	3.6
Bt5	164–250	10R 4/6	68.0	4.9	27.1	0.21	9.8	3.8	2.5
BC1	250–293	2.5YR 3/6	67.4	4.7	27.9	0.17	9.5	4.1	2.9
BC2	293–340	2.5YR 4/6	75.1	3.4	21.5	0.17	8.4	5.0	6.4
BC3	340–393	2.5YR 4/8	83.4	1.9	14.7	0.39	10.3	7.2	5.3
CB1	393–445	5YR 5/8	96.2	1.6	2.2	1.95	13.6	14.1	5.4
<i>A: sandy, siliceous, subactive, thermic Psammentic Paleudult</i>									
Ap	0–38	10YR 3/3	90.6	6.9	2.5	4.54	–	–	7.3
E	38–123	2.5YR 3/6	89.7	5.8	4.5	1.01	–	–	7.4
Bt	123–260	10R 4/6	84.5	3.4	12.1	0.19	8.7	7.2	8.1
BC1	260–370	10R 4/6	84.6	8.7	6.7	0.13	7.8	4.8	2.7
BC2	370–420	2.5YR 4/6 ^b	88.6	2.3	9.1	0.20	–	–	6.8
BC3	420–510	2.5YR 4/6 ^b	94.6	2.2	3.2	0.61	–	–	2.1
C1	510–720	2.5Y 6/8 ^b	97.3	0.5	2.3	0.00	–	–	6.7
<i>F: sandy, siliceous, subactive, thermic Psammentic Paleudult</i>									
Ap	0–25	10YR 3/3	89.8	7.6	2.6	4.80	–	–	2.9
E1	25–62	2.5YR 4/8	88.9	6.5	4.6	1.57	–	–	2.3
E2	62–126	5YR 4/6	89.6	6.1	4.3	2.10	–	–	3.9
Bt1	126–176	2.5YR 4/6	84.9	3.7	11.4	0.73	10.0	4.3	3.2
Bt2	176–240	2.5YR 4/6	89.4	2.8	7.8	0.90	6.5	6.9	5.6
BC1	240–305	10R 4/6	90.1	0.0	9.9	0.47	6.4	6.3	1.9
BC2	305–349	2.5YR 4/6	87.4	2.0	10.6	0.49	–	–	3.2
BC3	349–392	2.5YR 4/8	88.1	6.4	5.5	0.51	–	–	5.1
C1	392–422	2.5YR 4/8	96.3	0.9	2.8	0.00	–	–	13.2
C2	422–507	2.5YR 4/6	93.5	1.1	5.4	–	–	–	4.9
<i>G: loamy, kaolinitic, thermic Grossarenic Kandiuult</i>									
Ap	0–33	10YR 3/3	83.3	12.5	4.2	2.31	–	–	0.6

Table 1 (continued)

Horizon	Depth (cm)	Color	Sand (%)	Silt (%)	Clay (%)	Fe _o /Fe _d ratio per 100 g of clay	CEC (cmol _c kg ⁻¹)	ECEC clay (cmol _c kg ⁻¹)	VC sand (%)
E	33–105	2.5YR 4/8	86.2	7.3	6.5	0.97	—	—	2.9
Bt1	105–205	10R 4/6	74.2	4.4	21.4	0.26	8.4	5.4	4.6
Bt2	205–228	10R 4/8	64.2	4.9	30.9	0.15	4.6	2.2	3.2
Bt3	228–285	10R 4/8	75.5	3.0	21.5	0.20	6.6	3.5	3.2
BC1	285–382	10R 4/8	86.5	1.0	12.5	0.27	—	—	4.7
BC2	382–447	2.5YR 4/6	83.1	1.7	15.2	0.21	—	—	4.8
C1	447–502	10R 4/8 I	89.0	1.8	9.2	0.05	—	—	3.5
C2	502–580	10R 4/8 I	75.6	7.2	17.2	—	—	—	2.2
<i>H: sandy, kaolinitic, thermic Grossarenic Kandiudult</i>									
Ap	0–35	10YR 3/3	84.1	12.5	3.4	3.46	—	—	3.0
Bt1	35–100	2.5YR 3/6	80.9	10.5	8.6	0.83	—	—	3.6
Bt2	100–185	10YR 4/6	69.5	5.9	24.6	0.26	9.5	8.2	4.0
Bt3	185–260	10R 4/6	59.2	4.7	36.1	0.12	5.6	3.2	6.7
Bt4	260–300	10R 4/6	79.7	1.2	19.1	0.21	4.7	2.4	3.2
BC1	300–420	10R 4/8	95.8	0.5	3.7	0.80	—	—	5.9
BC2	420–510	10R 4/8	86.8	2.0	11.2	0.49	—	—	7.0
BC3	510–570	5YR 4/6 I	81.9	5.8	12.3	0.13	—	—	5.7
C1	570–690	2.5Y 8/1 I	10.8	29.3	59.9	0.10	—	—	1.2

^a Fe_o/Fe_d = oxalate-extractable Fe/dithionite–citrate–bicarbonate-extractable Fe per 100 g of clay; CEC = cation exchange capacity; ECEC = effective cation exchange capacity; very coarse (VC) sand (1–2 mm) is on a clay-free basis.

^b Colors and/or textures stratified.

Hajek (1982), using the ratios of HIV and quartz XRD peaks to an internal kaolinite standard (*d*-spacings of 1.40 nm for HIV, 0.72 nm for kaolinite, and 0.425 nm for quartz).

Oriented clods from the NW and SE pedons were air-dried and impregnated with thermal epoxy resin. Thin sections were made by standard techniques (Murphy, 1986).

3. Results and discussion

3.1. Soil distribution

All soils examined had sandy eluvial horizons of varying thickness overlying argillic horizons, and six of the 11 profiles possessed kandic horizons (Table 1 and Fig. 2). The five Paleudult pedons had subsurface diagnostic horizons too sandy for recognition of a kandic horizon. The soils examined are of two general types. The first consists of sandy A and E horizons overlying a loamy sand or light sandy loam argillic horizon. The argillic horizons in these soils contain <25% clay throughout and are referred to as sandy argillic horizons. The second type also consists of sandy eluvial horizons overlying loamy sand or sandy loam argillic horizons, but has a second clay increase to sandy clay loam with >25% clay; they are referred to as loamy argillic horizons, even though this nomenclature does not coincide with textural definitions in soil taxonomy. All pedons are in kaolinitic or

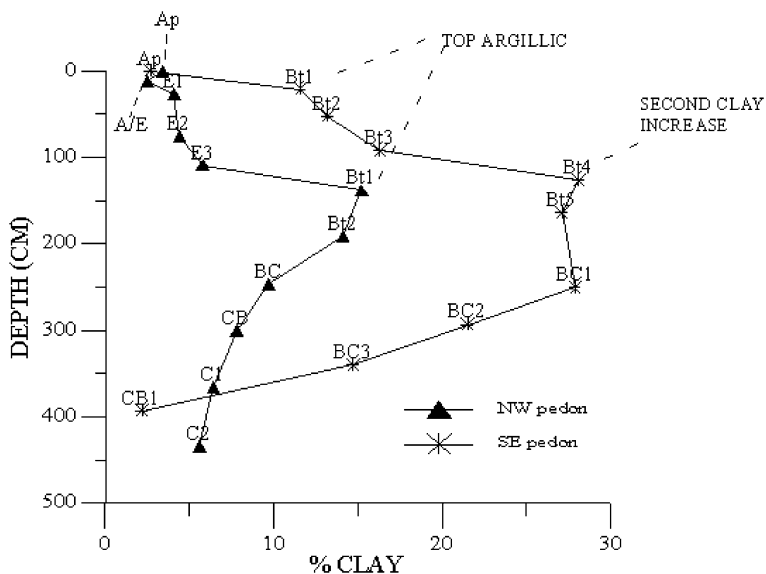


Fig. 3. Changes in clay concentration with depth for the NW and SE pedons.

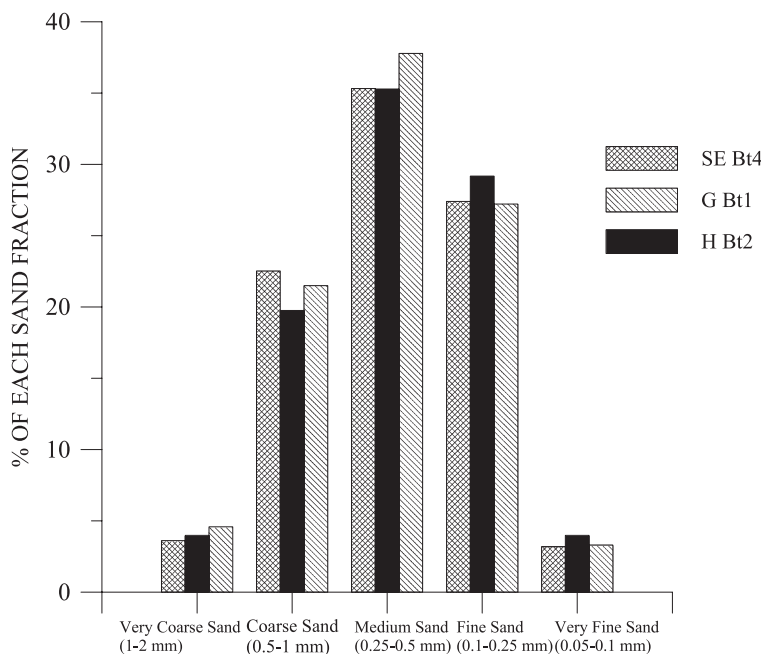


Fig. 4. Clay-free sand size distributions in the horizon below the abrupt clay increase in pedons SE, G, and H.

siliceous families, and are taxonomically separated (Fig. 2) by the texture of the subsurface diagnostic horizon and the thickness of sandy eluvial horizons. The southerly slope and the generally decreasing thickness of the sandy eluvial horizons at the southeastern end of the plot suggest that slight erosion has occurred.

3.2. Parent material differences between pedons

The pedons possessing >25% clay in part of the argillic horizon (SE, G, and H) are generally located toward the SE portion of the plot (Table 1, Fig. 2). In these pedons, horizons with sandy clay loam texture occur either in the upper part of the argillic horizon, or within the argillic horizon coincident with a second increase in clay (Bt4, Bt1, and Bt2, for SE, G, and H, respectively) (Table 1, Fig. 3). The depth to the sandy clay loam texture is 1.00–1.26 m below the soil surface, and the upper surface of this clay increase is generally flat (elevations of 129.1, 129.2, and 129.2 m for the SE, G, and H sites, respectively). This does not exactly reflect the ground surface topography (130.4, 130.3, and 130.2 for SE, G, and H, respectively), which might be expected of contemporary pedogenic features. The sand size distributions (on a clay-free basis) of horizons with sandy clay loam texture in the SE, G, and H pedons are similar (Fig. 4), suggesting that they are lithologically related. From this evidence, we suggest that the relatively large increases in clay within the argillic horizons are either depositional features, or result from clay illuviation related to a past geomorphic surface.

The upper boundary of the argillic horizon in all pedons generally slopes to the south (Fig. 5), and is approximately parallel to the present-day surface. A layer consisting

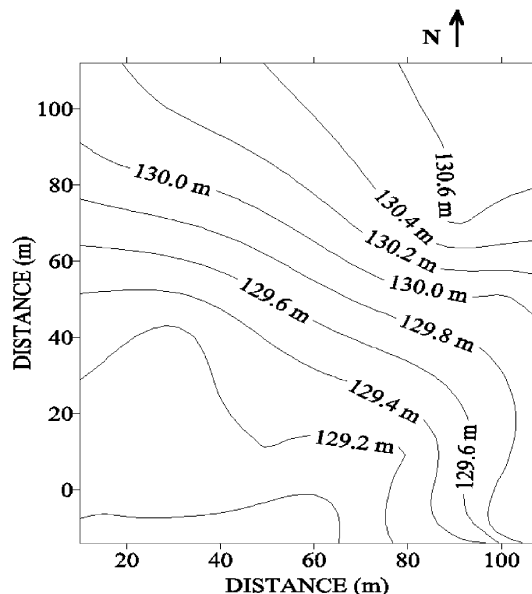


Fig. 5. The elevation of the upper boundary of the argillic horizon in the plot. Contour lines are at 0.2-m intervals.

dominantly of medium and fine sand occurs at 129.5-m (± 0.03 m) elevation in pedons E, F, G, and H, and a layer of predominantly medium sand is present in A, B, and D at 128.2 (± 0.07 m). The similar elevation of these two layers suggests that they are relatively continuous horizontal layers. The fact that the upper boundary of the argillic

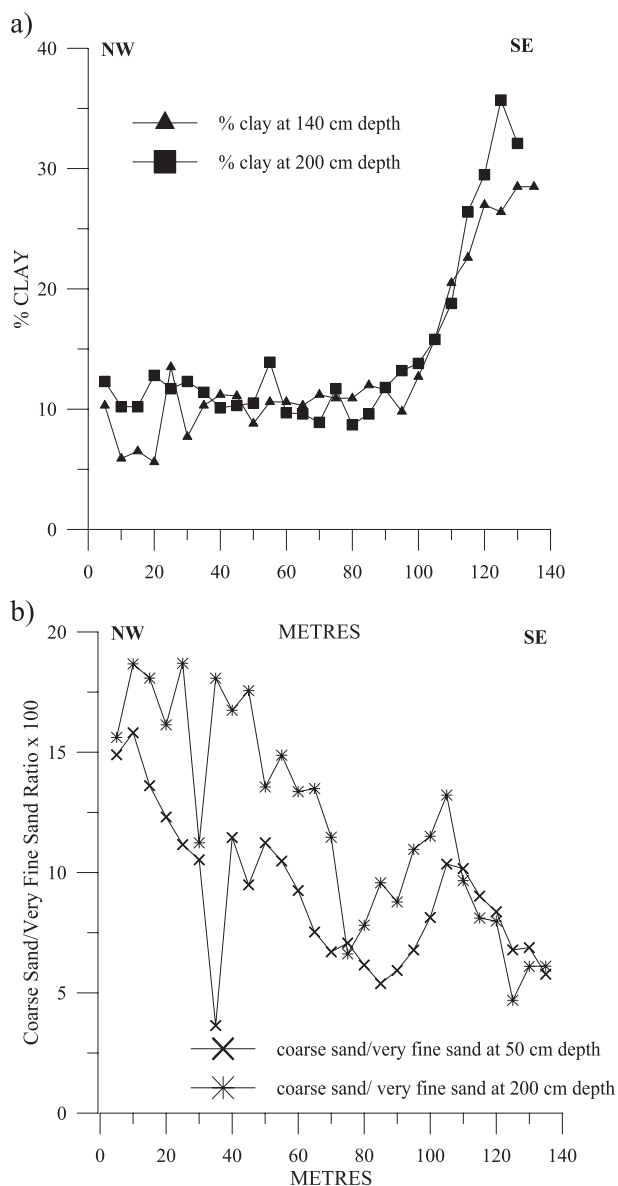


Fig. 6. (a) The clay concentration at two depths (140 and 200 cm) and (b) the ratio of coarse sand (0.5–1 mm) to very fine sand (0.05–0.1 mm) at 50 and 200 cm depths along the plot transect proceeding from NW to SE.

horizon is generally parallel to the ground surface suggests that formation of the argillic horizon is associated with the contemporary geomorphic surface.

The argillic horizon increases in clay content from northwest to southeast along the transect within the plot. At both 140 and 200 cm depths, the clay content increases fairly abruptly from northwest to southeast at 100–120 m along the transect (Fig. 6a). Differences in either weatherable minerals or clay illuviation could account for these lateral differences in clay, but it is unlikely that they would occur so abruptly. Sand fractions (0.05–2.0 mm) taken from the C horizons are almost entirely composed of quartz (data not shown), as also noted in similar landscapes of the North Carolina Coastal Plain by Gamble and Daniels (1974). Assuming similar amounts of weatherable minerals in these pedons, the differences in clay content probably result from differences in the parent material. Variations in the coarse sand (0.5–1 mm)/very fine sand (0.05–0.1 mm) ratio across the plot (Fig. 6b) also indicate lateral heterogeneity of parent materials.

Fine clay ($<0.2\ \mu\text{m}$)/coarse clay ($0.2\text{--}2.0\ \mu\text{m}$) ratios, often diagnostic for evaluating illuvial clay (Cabrera-Martinez et al., 1989), do not indicate differences in amounts of illuvial clay between the loamy and sandy argillic horizons (data not shown). They also do not vary with depth within the argillic horizon for the loamy pedons that exhibit two distinct increases in clay. Clay bridges observed in Bt horizons in the field were also identified in thin sections (Fig. 7a and b), but were not abundant. Some illuvial clay features may have been destroyed over time. Alternatively, the lack of better illuvial clay expression may be evidence that differences in the amount of clay in the argillic horizon result from parent material differences, rather than differences in weathering and translocation of colloidal silicates.

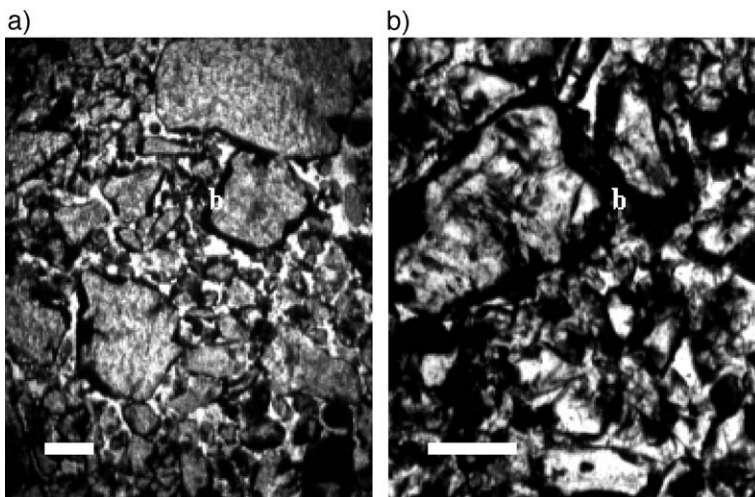


Fig. 7. Photomicrographs of thin sections from (a) the Bt1 horizon of profile SE under plane polarized light; and (b) the Bt1 horizon of profile NW under plane-polarized light; b = clay bridging. Bar = 1 mm.

3.3. Parent material differences within pedons

The plot of skewness vs. the coefficient of variation (CV) of the sand grain size distribution for horizons of the NW and SE pedons (Fig. 8a) suggest that differences in the mode of parent material deposition exist within pedons. There seems to be a group (lower left on the plot) corresponding to most horizons of the NW (Ap, A/E, E, and Bt horizons) and SE (Ap, Bt, and BC horizons) pedons, and another group (upper right on plot) corresponding to subjacent horizons (transitional to C and C horizons). Most horizons in the sola of both pedons are less positively skewed and better sorted than C horizons. The plot of kurtosis vs. the CV of the sand grain size distribution from the same horizons (Fig. 8b) suggests a similar break corresponding to the bottom of the solum, although other interpretations are also possible.

The plots illustrate that differences in sand grain distributions are mostly related to CV and, consequently, to sorting characteristics. The lower CVs of the grain size distributions exhibited by most of the horizons within the sola indicate slightly better sorting in the upper portions of the profiles. In addition, the lower horizons tend to exhibit more positive skewness values. Friedman (1961, 1979) proposed that most river and eolian sands are positively skewed because of preferential transport of finer particles in the suspended load. The increased skewness with depth suggests that the lower horizons have a greater fluvial or eolian component than the near-surface horizons. Medium sand/fine sand ratios in the NW and SE profiles increase at 2–4 m depth in the lower Bt and BC horizons (Fig. 9). These depths are similar to the breaks in the groupings shown on the skewness and kurtosis plots (e.g., the Bt2/BC boundary for

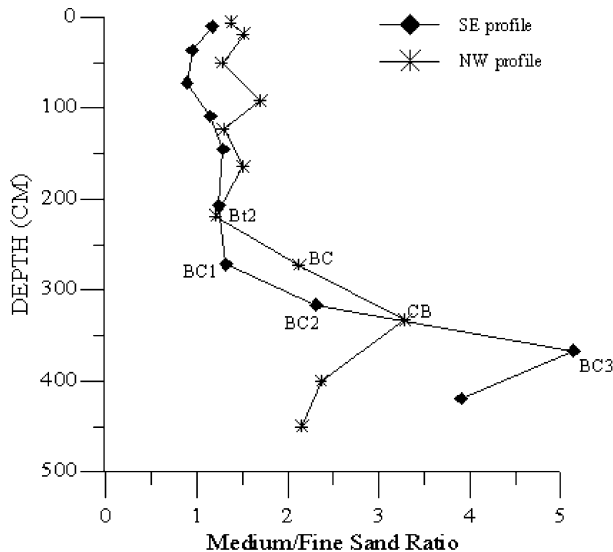


Fig. 9. Vertical distribution of medium sand (0.25–0.5 mm)/fine sand (0.1–0.25 mm) ratios for the NW and SE profiles.

NW; the BC1/BC2 boundary for SE). These data suggest the presence of two parent materials in these pedons, the discontinuity between them occurring close to the bottom of the solum. As reported by Gamble et al. (1969) and Leigh (1998), we did not find evidence for a discontinuity between the eluvial and illuvial horizons. In addition, the medium sand/fine sand ratio is not the same from pedon to pedon, again indicating lateral variability of parent materials in this landscape.

3.4. Possible eolian influence

Separations based on graphical presentations of moments have been developed for eolian and fluvial sediments (Friedman, 1979; Leigh, 1998). The empirical differences indicate that eolian sediments are finer (higher mean) and better sorted (lower standard deviation) than fluvial sediments. Fig. 10 shows the mean and standard deviation values for the NW and SE samples and the breaks between fluvial and eolian deposits proposed by Friedman (1979) and Leigh (1998). Horizons on the left side of the graph contain the relatively coarser and less well sorted sand grains, which we suggest were deposited by fluvial mechanisms, whereas horizons on the right side of the graph are composed of sand that we suggest is eolian because it is better sorted and finer. The solid line roughly corresponds with the breaks between the solum (eolian) and underlying BC and C (fluvial) horizons. In the region, eolian dunes occur predominantly on the eastern side of rivers (Markewich and Markewich, 1994), suggesting that the source area for these

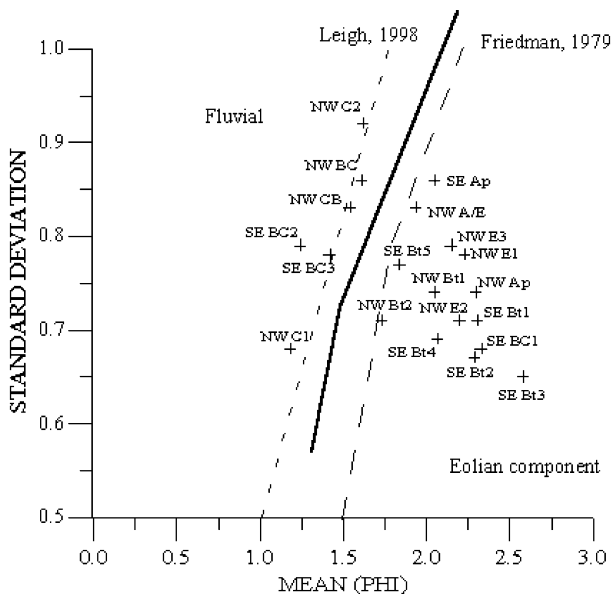


Fig. 10. Standard deviation of ϕ vs. the mean ϕ sand grain size from the NW and SE pedons. Dashed lines are those of Leigh (1998) and Friedman (1979) for the boundaries between fluvial and eolian sands. The solid line roughly corresponds with the breaks between the solum and underlying BC and C horizons.

olian sands was associated with Ty Ty Creek. However, the location of possible source areas for eolian contributions is beyond the scope of this paper; it was considered by Daniels (1969).

Fig. 10 suggests that upper horizons of the profiles have an eolian component, whereas the lower horizons are fluvially derived. However, the solum possesses some sand, which is coarser than expected for completely eolian derived materials, as its first percentile (ϕ_1) is >1 mm (Leigh, 1998). Upper horizons in most of the pedons have $>2\%$ very coarse sand (1–2 mm diameter) in the solum (Table 1), and this precludes a completely eolian origin. In addition, the high clay content of the SE solum does not fit a completely eolian origin. In a similar landscape, Leigh (1998) deduced that the surficial sands at five of six sites on terraces and interfluvies in the Sand Hills of South Carolina were of fluvial origin. Because of the presence of buried Native American artifacts, Leigh (1998) originally proposed that the artifacts had been buried by eolian sediment. However, he later concluded that these sites had been subjected to bioturbation resulting in burial of the artifacts. Similarly, it is possible that eolian additions to these soils have been mixed with a fluvial matrix, thus giving mixtures of both eolian and fluvial sediment in the upper horizons. Bioturbation could result in complete mixing of much of the upper portions of a soil. Alternatively, these sediments may have been mixed by shallow fluvial reworking after eolian deposition, which would also yield sediment of mixed characteristics.

3.5. Weathering trends

Subaerial exposure and subsequent weathering of primary minerals in humid, warm environments often lead to the formation of kaolinite, HIV, Fe oxides, and gibbsite in the clay fraction (Karathanasis et al., 1983). Reddish hues (10 R, 2.5 YR) throughout the sola of the profiles indicate a relatively weathered and highly oxidized status (Table 1). For all subsoils examined, XRD analyses show that kaolinite, gibbsite, and HIV are the dominant minerals in the clay (<2 μm) fraction.

We attempted to assess differences in weathering or pedogenesis between the pedons by examining (1) extractable Fe forms, (2) HIV quantities, and (3) gibbsite/kaolinite ratios in the clay fraction. The rationale was that the greater is the degree of weathering, the more pedogenic is the formation of gibbsite at the expense of kaolinite (enhanced Si loss). Although gibbsite can form rapidly in environments with a large portion of weatherable minerals (Norfleet and Smith, 1989), we interpret higher gibbsite/kaolinite ratios in this environment to indicate enhanced Si loss and advanced weathering.

Ratios of Fe_o/Fe_d (expressed on a 100-g-of-clay basis) do not vary much between the soils (Table 1). The HIV quantities generally decrease with depth, but are approximately the same in the NW and SE pedons (Fig. 11a). The ratio of gibbsite/kaolinite generally decreases with depth (Fig. 11b), and the soils with loamy argillic horizons (SE, H, and G) tend to have lower gibbsite/kaolinite ratios than the soils with sandy argillic horizons (NW, B and F), suggesting a greater degree of Si leaching in the sandy soils. This implies increased weathering. Consequently, these results suggest that soils with loamier argillic horizons are less weathered than the sandier soils. The effective saturated hydraulic conductivity (weighted mean for the entire solum down to the CB horizons)

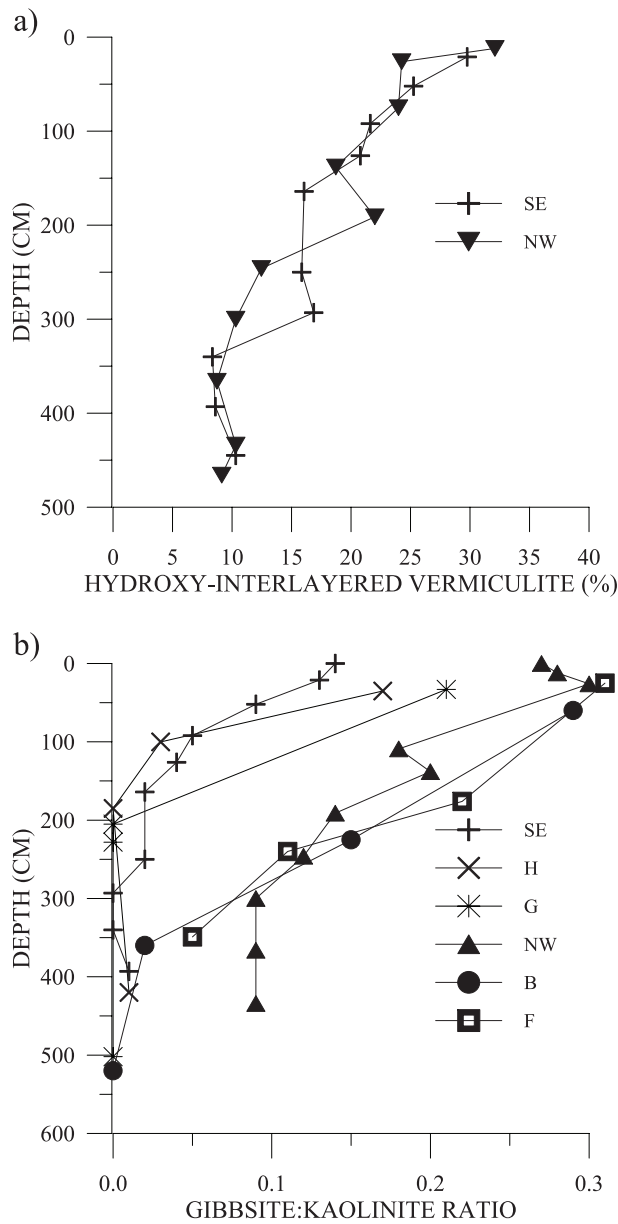


Fig. 11. (a) Hydroxy-interlayered vermiculite quantities in the NW and SE pedons. (b) Gibbsite/kaolinite ratios for selected pedons. The SE, H, and G pedons have loamy subsoils and the NW, B, and F pedons possess sandy subsoils.

measured with the borehole technique (Amoozegar, 1989) for the sandy NW pedon is almost five times greater (35.2 cm h^{-1}) than that of the loamy SE pedon (7.5 cm h^{-1}). This would cause more intensive leaching and increased loss of Si for these sandier pedons.

4. Conclusions

Differences in soil properties across this plot are related to differences in the parent materials, which seem to control the amount of clay present in argillic horizons. Two parent materials are present in the profiles, and the lower boundary of the argillic horizon corresponds approximately with the discontinuity. There is probably an eolian component in the upper portion of the profile, most likely derived from wind erosion of sands along Ty Ty Creek. In similar soils of the region (other Arenic and Grossarenic soils), horizontal discontinuities have rarely been identified (Gamble et al., 1969; Leigh, 1998), and we were surprised to find the discontinuities. However, discontinuities are not evident between eluvial and illuvial horizons, but are located deeper in the illuvial portion of the solum.

As suggested by Gamble and Daniels (1974) for the North Carolina Coastal Plain, parent material is a major determinant of soil properties. They speculated that ultisols with strongly weathered mineralogical suites are the only soils that could form in the parent materials present in the Upper and Middle Coastal Plain of the southeastern USA. We agree with this and also suggest that parent materials control soil formation to a finer scale in these settings, in particular dictating subsoil clay quantities that determine soil family placement in US Soil Taxonomy. Although terrain attributes are similar (geomorphic component, slope, and aspect), large differences in soils and accessory properties (water-holding capacity, nutrient retention, and rooting depth) result from parent material variation across these landscapes.

References

- Amoozegar, A., 1989. A compact constant-head permeameter for measuring saturated hydraulic conductivity of the vadose zone. *Soil Sci. Soc. Am. J.* 53, 1356–1361.
- Asmussen, L.E., 1971. Hydrologic effects of Quaternary sediments above the marine terraces in the Georgia coastal plain. *Southeast. Geol.* 12, 189–201.
- Bosch, D.D., West, L.T., 1998. Hydraulic conductivity variability for two sandy soils. *Soil Sci. Soc. Am. J.* 62, 90–98.
- Bui, E.N., Mazzullo, J.M., Wilding, L.P., 1989. Using quartz grain size and shape analysis to distinguish between eolian and fluvial deposits in the Dallal Bosso of Niger (West Africa). *Earth Surf. Processes Landf.* 14, 157–166.
- Cabrera-Martinez, F., Harris, W.G., Carlisle, V.W., Collins, M.E., 1989. Evidence for clay translocation in coastal plain soils with sandy/loamy boundaries. *Soil Sci. Soc. Am. J.* 53, 1108–1114.
- Daniels, R.B., 1969. Eolian sands associated with Coastal Plain River Valleys—some problems in their age and source. *Southeast. Geol.* 11, 97–110.
- Daniels, R.B., Gamble, E.E., Cady, J.G., 1970. Some relations among coastal plain soils and geomorphic surfaces in North Carolina. *Soil Sci. Soc. Am. Proc.* 34, 648–653.

- Davis, R.A., 1992. *Depositional Systems: An Introduction to Sedimentology and Stratigraphy*. Prentice Hall, New Jersey.
- Drever, J.I., 1973. The preparation of oriented clay mineral specimens for X-ray diffraction analysis by a filter membrane peel technique. *Am. Mineral.* 58, 553–554.
- Friedman, G.M., 1961. Distinction between dune, beach, and river sands from their textural characteristics. *J. Sediment. Petrol.* 31, 514–529.
- Friedman, G.M., 1979. Differences in size distributions of populations of particles among sands of various origins. *Sedimentology* 26, 3–32.
- Gamble, E.E., Daniels, R.B., 1974. Parent material of upper and middle coastal plain soils in North Carolina. *Soil Sci. Soc. Am. Proc.* 38, 633–637.
- Gamble, E.E., Daniels, R.B., McCracken, R.J., 1969. A2 horizons of coastal plain soils: pedogenic or geologic origin. *Southeast. Geol.* 11, 137–152.
- Green, P., 1974. Recognition of sedimentary characteristics in soils by size–shape analysis. *Geoderma* 11, 181–193.
- Jackson, M.L., 1975. *Soil Chemical Analysis—Advanced Course*. M.L. Jackson, Madison, WI.
- Jackson, M.L., Lim, C.H., Zelazny, L.W., 1986. Oxides, hydroxides, and aluminosilicates. In: Klute, A. (Ed.), *Methods of Soil Analysis: Part 1. Physical and Mineralogical Methods*, 2nd ed. Agronomy Monograph, vol. 9. ASA and SSSA, Madison, WI, pp. 113–119.
- Karathanasis, A.D., Hajek, B.F., 1982. Revised methods for quantitative determination of minerals in soil clays. *Soil Sci. Soc. Am. J.* 46, 419–425.
- Karathanasis, A.D., Adams, F., Hajek, B.F., 1983. Stability relationships in kaolinite, gibbsite, and Al-hydroxy interlayered vermiculite soil systems. *Soil Sci. Soc. Am. J.* 47, 1247–1251.
- Kilmer, V.J., Alexander, L.T., 1949. Methods of making mechanical analysis of soils. *Soil Sci.* 68, 15–24.
- Leigh, D.S., 1998. Evaluating artifact burial by eolian versus bioturbation processes, South Carolina Sandhills, USA. *Geoarchaeology* 13, 309–330.
- Markewich, H.W., Markewich, W., 1994. An overview of Pleistocene and Holocene inland dunes in Georgia and the Carolinas—morphology, distribution, age, and paleoclimate. *USGS Tech. Bull.*, 2069.
- Markewich, H.W., Pavich, M.J., Mausbach, R.L., Hall, R.G., Hearn, P.P., 1986. Age relations between soils and geology in the coastal plain of Maryland and Virginia. *USGS Tech. Bull.*, 1589-A.
- Mazzulo, J.M., Ehrlich, R., 1983. Grain-shape variation in the St. Peter sandstone: a record of eolian and fluvial sedimentation of an early Paleozoic cratonic sheet sand. *J. Sediment. Petrol.* 53, 105–119.
- Murphy, C.P., 1986. *Thin Section Preparation of Soils and Sediments*. AB Academic Publishers, Berkhamsted, Herts, UK.
- Norfleet, M.L., Smith, B.R., 1989. Weathering and mineralogical classification of selected soils in the Blue Ridge Mountains of South Carolina. *Soil Sci. Soc. Am. J.* 53, 1771–1778.
- Rebertus, R.A., 1998. Loessial soils of Delaware: taxonomy and map-unit assessment. *Soil Sci. Soc. Am. J.* 62, 412–422.
- Schoeneberger, P.J., Wysocki, D.A., Benham, E.C., Broderson, W.D., 1998. *Field book for describing and sampling soils*. Natural Resources Conservation Service, USDA National Soil Survey Center, Lincoln, NE.
- Soil Survey Investigations Staff, 1996. *Soil survey laboratory methods manual*. Soil Survey Investigations Report, vol. 42. USDA-SCS, National Soil Survey Center, Lincoln, NE.
- Tan, K.H., Hajek, B.F., Barshad, I., 1986. Thermal analysis techniques. In: Klute, A. (Ed.), *Methods of Soil Analysis: Part 1. Physical and Mineralogical Methods*, 2nd ed. Agronomy Monograph, vol. 9. ASA and SSSA, Madison, WI, pp. 151–183.
- Whittig, L.D., Allardice, W.R., 1986. X-ray diffraction techniques. In: Klute, A. (Ed.), *Methods of Soil Analysis: Part I. Physical and Mineralogical Methods*, 2nd ed. Agronomy, vol. 9. ASA and SSSA, Madison, WI, pp. 336–341.
- Zhu, A.X., Band, L., Vertessy, R., Dutton, B., 1997. Derivation of soil properties using a Soil Land Inference Model (SoLIM). *Soil Sci. Soc. Am. J.* 61, 523–533.